In Situ NMR of SAPO-34 Crystallization

Ørnulv B. Vistad,[†,‡] Duncan E. Akporiaye,[‡] Francis Taulelle,*[,§] and Karl Petter Lillerud[†]

University of Oslo, P.O. Box 1033, Blindern, 0315 Oslo, Norway, SINTEF Applied Chemistry, P.O. Box 124, Blindern, 0314 Oslo, Norway, and RMN et Chimie du Solide, Tectonique Moléculaire du Solide FRE 2423 CNRS, Université Louis Pasteur, 4 rue Blaise Pascal, Strasbourg Cedex, France

Received September 24, 2002. Revised Manuscript Received January 8, 2003

SAPO-34 (SAPO: silicoaluminophosphate) has been synthesized and examined by in situ multinuclear high-resolution NMR under hydrothermal conditions (170 °C) in the presence of HF, using morpholine as the structure-directing agent. Four routes have been examined: (a) from a SAPO gel with HF (triclinic SAPO-34), (b) from a SAPO gel without HF (trigonal SAPO-34), (c) from an $AlPO_4$ gel with HF (triclinic $AlPO_4$-34), and (d) from a slurry containing the layered $AlPO_4F$ prephase (triclinic $AlPO_4$-34). In situ ^{13}C, ^{19}F, ^{27}Al, and ^{31}P NMR have uncovered the main steps of the reaction. The gel dissolves into small units condensed to no more than 4-rings (4R). The next steps are formation of a layered intermediate (the prephase), redissolution of the prephase into 4R building units of different types depending on the fluoride contents and aluminum coordination, and the subsequent nucleation and crystallization of triclinic $AlPO_4$/SAPO-34. The initial fast process leads to the formation of the prephase made of an alternating stacking of 4R type-II units. When approaching 170 °C, this phase redissolves in 4R type-III units with aluminum in five-coordination. With additional defluorination, 4R type-IV units transform into 4R type-V units and both types connect in a chabazite topology. One 4R type-IV unit clips two fluorine atoms into the bridging position in the 4-ring and subsequently shapes the network topology into its crystalline order. The mechanism provided can now be subjected to further chemical testing for purposes of syntheses optimization.

Introduction

The demand for new functional porous materials with higher selectivity in separation technologies and higher selectivity and rates of conversion in the fine chemical and catalysis industry is continuously increasing. However, despite the growing number of new structures/materials, the preparation, which involves hydrothermal crystallization from a supersaturated solution, is still a poorly understood process because of the complexity of the gels. The key to controlling the formation of the crystalline microporous material resides in a fundamental understanding of the processes leading to and sustaining nucleation and subsequent crystal growth under hydrothermal conditions. Much knowledge has been accumulated during the past decade, but much research remains to be done before rational design of new materials with targeted properties (composition, size, morphology, shape selectivity, acidity, etc.) would be achievable.

Microporous materials such as $AlPO_4$s and SAPOs (silicoaluminophosphates) were first synthesized in 1982 by Flanigen and co-workers.[1,2] Since their discovery, some important industrial applications have been developed, particularly the use of SAPO-34 as a shape-selective catalyst for the conversion of methanol to olefins in the MTO process.[3−8]

In many studies, batch-mode techniques have been undertaken to investigate hydrothermal crystallization. The crystallization is then terminated by quenching of the reaction at different stages. The outcome is examined by a variety of ex situ techniques in an attempt to gain a detailed understanding of the processes taking place during the synthesis. These ex situ methods, although providing useful information, cannot provide a complete picture of the processes occurring under reaction conditions. The chemistry at high temperatures

* Corresponding author. E-mail: taulelle@chimie.u-strasbg.fr.
† University of Oslo.
‡ SINTEF Applied Chemistry.
§ Université Louis Pasteur.

(1) (a) Wilson, S. T.; Lok, M. B.; Messina, C. A.; Cannan, T. R.; Flanigen, E. M. *J. Am. Chem. Soc.* **1982**, *104*, 1146. (b) Wilson, S. T.; Lok, M. B.; Messina, C. A.; Cannan, T. R.; Flanigen, E. M. U.S. Patent 4,310,440, Jan 12, 1982.

(2) (a) Lok, M. B.; Messina, C. A.; Patton, R. L.; Gajek, R. T.; Cannan, T. R.; Flanigen, E. M. *J. Am. Chem. Soc.* **1984**, *106*, 6092. (b) Lok, M. B.; Messina, C. A.; Patton, R. L.; Gajek, R. T.; Cannan, T. R.; Flanigen, E. M. U.S. Patent 4,440,871, April 3, 1984.

(3) Støcker, M.; Weitkamp, J. *Microporous Mesoporous Mater.* **1999**, *8*, 1.

(4) Anderson, M. W.; Sulikowski, B.; Barrie, B. J.; Klinowski, J. *J. Phys. Chem.* **1990**, *94*, 2730.

(5) Wendelbo, R.; Akporiaye, D. E.; Andersen, A.; Dahl, I. M.; Mostad, H. B. *Appl. Catal. A* **1996**, *142*, L197.

(6) Dahl, I. M.; Kolboe, S. *Catal. Lett.* **1993**, *20*, 329.

(7) *Natural Gas Conversion IV. Studies in Surface Science and Catalysis*; dePontes, M., Espinoza, R. L., Nicolaides, C. P., Scholtz, J. H., Scurell, M. S., Eds.; Elsevier: Amsterdam, 1997; Vol. 107, p 87.

(8) Barger, P. T.; Wilson, S. T. *Proceedings of the 12th International Zeolite Conference*, Baltimore, 1998; Treacy, M. M. J., Marcus, B. K., Bisher, M. E., Higgins, J. B., Eds.; Materials Research Society: Warrendale, PA, 1998; Vol. 1, p 567.

10.1021/cm021317w CCC: $25.00
Published on Web 03/29/2003

and autogenous pressures is most likely quite different from room-temperature chemistry. The dielectric constant of water, which acts as the solvent in the systems under investigation, is significantly reduced when the temperature and pressure are increased (from ca. 80 at 20 °C and 1 bar to about 38 at 180 °C and 10 bar),[9] implying a reduced polarizing power of the solvent. Another aspect observed during synthesis of $AlPO_4$s in the weak acidic pH range is a change in coordination of aluminum induced by temperature.[10,11] These differences reduce the pertinence of batch-mode techniques only (extrapolation from room temperature to high temperature), and formation of the critical intermediates may very well be missed.

Throughout the past decade, an increasing number of in situ studies of the formation of micro- and mesoporous materials have been reported.[12] The two most important techniques are synchrotron powder X-ray diffraction[12−16] and NMR,[10,11,17−19] but light scattering,[20] neutron diffraction,[21,22] SAXS and SANS,[23] EXAFS,[24] ESR,[25] and diffuse reflectance IR spectroscopy[25] have been shown to be useful as well. The NMR is unique as a method for investigating microporous materials formation because one can gain detailed information concerning the speciation of atomic environments in the solid and liquid phases formed as well as their relative concentrations in the heterogeneous medium. Coupling NMR and XRD appears especially powerful for mechanistic elucidation.

In this study, in situ (^{13}C, ^{19}F, ^{27}Al, and ^{31}P) NMR has been applied to real time investigation of the crystallization of SAPO-34 under hydrothermal conditions, in the presence of HF, using morpholine as the structure-directing agent (SDA).[26−29] Despite the special interest that has been devoted to SAPO-34 for the MTO process, its mechanism of formation is still an open question. The NMR spectra are assigned according to NMR studies of model solutions.[30−43] One disadvantage with most of these studies is that $Al(NO_3)_3$ or $AlCl_3$ is used as an Al source, giving clear solutions in the low-pH region, which is not strictly comparable to the $AlPO_4$/SAPO-gel syntheses.

Background From the in Situ Powder X-ray Diffraction Study. The results of this study are strongly linked to the in situ powder X-ray diffraction investigation of the same system published previously.[44] Its main results are summed up as follows. When linear heating (2 °C/min) was used, formation of a crystalline intermediate precursor (named the prephase) was observed by in situ X-ray powder diffraction when the temperature reached ∼95 °C.[44] The prephase is built up of $AlPO_4F$ slabs separated by a double layer of protonated morpholine molecules located in an ordered fashion between the slabs ($a = 14.473$ Å, $b = 6.930$ Å, $c = 9.239$ Å, and $\beta = 101.54°$). The prephase can easily be formed and separated as a pure phase at intermediate synthesis temperatures (∼125 °C). It contains variable amounts of silicon depending on the synthesis time of the prephase, and it was demonstrated that the prephase is of critical importance for obtaining SAPO-34 under the conditions studied by in situ XRD.[44] In addition, a single unassigned reflection at low angles was observed during the conversion of the prephase to the final triclinic SAPO-34 phase.

When the prephase was used as the starting material with the addition of water, triclinic $AlPO_4$-34 (Si-free) was obtained after hydrothermal treatment at 180 °C for 24 h. Thus, the prephase contained all the species necessary to produce $AlPO_4$-34 with the CHA topology.

Experimental Section

Chemicals and Mixing Procedures. SAPO-34 could be prepared in the presence and the absence of hydrofluoric acid using essentially the same final gel composition: 2.1:1.0:1.0:1.0:*x*:60 morpholine:SiO_2:Al_2O_3:P_2O_5:HF:H_2O (molar ratio). In this study, the focus was primarily devoted to the fluoride-containing system by adding 1 equiv of HF, which shows faster nucleation and crystal growth.[26,44] The mixtures were prepared by first mixing one-fourth of the deionized water with phos-

(9) Archer, D. G.; Wang, P. *J. Phys. Chem. Ref. Data* **1990**, *19*, 371.
(10) Taulelle, F.; Haouas, M.; Gerardin, C.; Estournes, C.; Loiseau, T.; Ferey, G. *Colloids Surf., A* **1999**, *158*, 299.
(11) Haouas, M. Etude RMN de la synthèse hydrothermales des aluminophosphate microporeux oxyfluorés: $AlPO_4$, CJ2, ULM-3 et ULM-4. Thèse, Université Louis Pasteur, Strasbourg, France, Jan 1999.
(12) Cheetham, A. K.; Mellot, C. F. *Chem. Mater.* **1997**, *9*, 2269.
(13) Chung, D. D. L.; De Haven, P. W.; Arnold, H.; Ghosh, D. *X-ray diffraction at elevated temperatures: A method for in situ process analysis*; VCH Publishers Inc.: New York, 1993; Chapter 7.
(14) Francis, R. J.; O'Hare, D. *J. Chem. Soc., Dalton Trans.* **1998**, 3133.
(15) Walton, R. I.; O'Hare, D. *Chem. Commun.* **2000**, 2283.
(16) Millange, F.; Walton, R. I.; Guillou, N.; Loiseau, T.; O'Hare, D.; Ferey, G. *Chem. Mater.* **2002**, *14*, 4448.
(17) Shi, J.; Anderson, M. W.; Carr, S. W. *Chem. Mater.* **1996**, *8*, 369.
(18) Haouas, M.; Gérardin, C.; Taulelle, F.; Estournes, C.; Loiseau, T.; Ferey, G. *J. Chim. Phys.* **1995**, *95*, 302.
(19) Gerardin, C.; Haouas, M.; Lorentz, C.; Taulelle, F. *Magn. Reson. Chem.* **2000**, *38*, 429.
(20) Schoeman, B. J. *Zeolites* **1997**, *18*, 97.
(21) Walton, R. I.; Smith, R. I.; O'Hare, D. *Microporous Mesoporous Mater.* **2001**, *48*, 79.
(22) Cheetham, A. K.; Wilkinson, A. P. *Angew. Chem., Int. Ed. Engl.* **1992**, *31*, 1557.
(23) Watson, J. N.; Iton, L. E.; White, J. W. *Chem. Commun.* **1996**, 2767.
(24) Landron, C.; Odier, Ph.; Bazin, D. *Europhys. Lett.* **1993**, *21*, 859.
(25) Weckhuysen, B.; Baetens, D.; Schoonheydt, R. A. *Angew. Chem., Int. Ed.* **2000**, *39*, 3419.
(26) Vistad, Ø. B.; Hansen, E. W.; Akporiaye, D. E.; Lillerud, K. P. *J. Phys. Chem. A* **1999**, *103*, 2540.
(27) Praksch, A. M.; Unnikrishnam, S. *J. Chem. Soc., Faraday Trans.* **1994**, *90*, 2291.
(28) Marchese, L.; Frache, A.; Gianotti, E.; Martra, G.; Causà, M.; Coluccia, S. *Microporous Mesoporous Mater.* **1999**, *30*, 145.
(29) Ashtekar, S.; Chilukuri, S. V. V.; Chakrabarty, D. K. *J. Phys. Chem.* **1994**, *98*, 4878.
(30) Sur, S. K.; Bryant, R. G. *Zeolites* **1996**, *16*, 118.
(31) Martinez, E. J.; Girardet, J.-L.; Morat, C. *Inorg. Chem.* **1996**, *35*, 706.
(32) Karlik, S. J.; Elgavish, G. A.; Pillai, R. P.; Eichhorn, G. L. *J. Magn. Reson.* **1982**, *49*, 164.
(33) Akitt, J. W.; Greenwood, N. N.; Lester, G. D. *J. Chem. Soc.* **1971**, 2450.
(34) Feng, Q.; Waki, H. *Polyhedron* **1991**, *10*, 659.
(35) Wilson, M. A.; Collin, P. J.; Akitt, J. W. *Anal. Chem.* **1989**, *61*, 1253.
(36) Mortlock, R. F.; Bell, A. T.; Radke, C. J. *J. Phys. Chem.* **1993**, *97*, 767.
(37) Mortlock, R. F.; Bell, A. T.; Radke, C. J. *J. Phys. Chem.* **1993**, *97*, 775.
(38) Miyajima, T.; Maki, H.; Kodama, H.; Ishiguro, S.-I.; Nariai, H.; Motooka, I. *Phosphorus Res. Bull.* **1996**, *6*, 281.
(39) Prasad, S.; Chen, W.-H.; Liu, S.-B. *J. Chin. Chem. Soc.* **1992**, *42*, 537.
(40) Prasad, S.; Liu, S.-B. *Microporous Mater.* **1995**, *4*, 391.
(41) Prasad, S.; Liu, S.-B. *Chem. Mater.* **1994**, *6*, 633.
(42) He, H.; Klinowski, J. *J. Phys. Chem.* **1994**, *98*, 1192.
(43) Marcuccilli-Hoffner, F. Etude des milieux de synthese floures de zeolithes et d'aluminophosphates microporeux. Thèse, Université de Haute Alsace, Mulhouse, France, 1992.
(44) Vistad, Ø. B.; Akporiaye, D. E.; Lillerud, K. P. *J. Phys. Chem. B* **2001**, *105*, 12437.

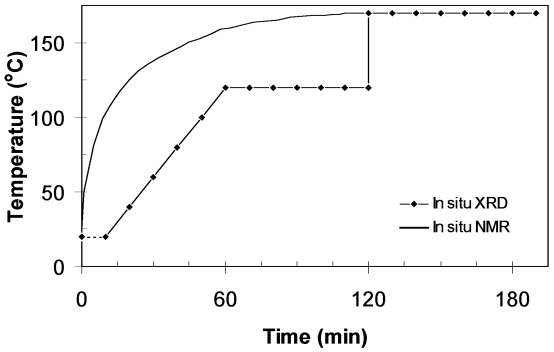

Figure 1. Heating profiles used in the in situ NMR and the in situ XRD study of SAPO-34 formation.

phoric acid (85 wt %, Merck) together with the aluminum source (Catapal-B, Vista Chemicals). The mixture, labeled solution A, was then stirred well before further addition of one-fourth of deionized water. Solution B was prepared by mixing Ludox LS-30 (Du Pont), morpholine (Acros Organics), and another one-fourth of the water. This solution was then slowly added to solution A with intense mixing, before the last one-fourth of the water was added. Subsequently, 1 equiv of 40 wt % HF (Fluka) was added at the end of the preparation. In the absence of HF, the synthesis time and temperature in ordinary Teflon-lined steel autoclaves was 48 h and 200 °C. In the presence of HF, the synthesis could be terminated after only 4−6 h. Additionally, a suspension containing 1.0 g of prephase and 5.2 g of water was prepared and examined by in situ ^{13}C, ^{27}Al, and ^{31}P NMR.

Two different synthesis techniques were applied: (a) In situ syntheses were carried out in the hydrothermal NMR tube (described below). (b) Due to the large differences between the in situ NMR tube and ordinary laboratory autoclaves (volume, shape, temperature gradients, heating profile, etc.), reference syntheses were performed in 50-mL Teflon-lined steel autoclaves at 170−190 °C. XRD patterns of the products obtained from the NMR tube and the steel autoclave syntheses were compared to ensure that synthesis conditions in the NMR experiments were comparable to the autoclave syntheses.

Characterization

NMR. Hydrothermal in situ ^{13}C, ^{19}F, ^{27}Al, and ^{31}P high-resolution NMR spectra were recorded on an MSL300 Bruker spectrometer at temperatures up to 170 °C. The syntheses were carried out in a specially made high-pressure Vespel tube (10-mm o.d., 8-mm i.d.) developed by Taulelle and co-workers.[10,45] The tube can withstand temperatures up to 250 °C and a pressure of ∼50 bar. A Teflon liner protects the Vespel tube from aggressive reagents common to zeolite syntheses, including HF, organic amines, and highly alkaline or acidic solutions. All the tube materials exhibit diamagnetic properties and are transparent to r.f. waves. A Bruker VT3000 variable-temperature unit was used to regulate the heating airflow. The actual internal temperature of the sample was calibrated using the ethylene glycol proton NMR method,[46] and the heating profile was measured by introducing a Copper−Constantan thermocouple (type T) into an open hydrothermal tube filled with Kryotox oil during a heating/cooling sequence (Figure 1). Signal intensity (area) was determined by numerical integration of the resonance peak or by spectrum fitting analysis when severe overlap of peaks was observed.

The ^{19}F chemical shifts were referenced to pure $CFCl_3$ using the peak from C_6F_6 at −163 ppm as an external secondary reference. The ^{13}C, ^{27}Al, and ^{31}P NMR chemical shifts were referenced to TMS, 1.0 M $Al(NO_3)_3$, and 85 wt % H_3PO_4 standard solutions, respectively. Due to the short synthesis time, and the low sensitivity of ^{29}Si, imposing long acquisition time, ^{29}Si NMR has not been acquired.

Three corrections compensate for intensity loss when increasing the temperature:[19] (a) corrections correlated to the Curie's law (the magnetization varies as $1/T$), (b) the filling volume (density of the sample varies with temperature), and (c) an estimated correction for loss due to changes in the electrical conductivity and dielectric constant of the sample that affects the loss factor of the probe. As an estimate of the variations of the gel density, tabulated values of the density changes of water as a function of temperature may be used. However, even if the hydrothermal NMR tube was constructed to reduce convection, small temperature gradients introduce flows of gas bubbles that add to the quantification difficulties. Additionally, colloidal particles invisible to NMR may be present in the sample volume. Corrections that affect the quality factor of the probe were not performed, assuming small changes in dielectric variations of the medium during synthesis. Thus, only intensity compensations for the Curie's law have been carried out and absolute intensity values were not actually measured in the present work. Nevertheless, the general trends are clearly visualized by the time and temperature variations of the NMR spectra.

Ex Situ pH Measurements. They were performed with an Orion 420A pH meter equipped with a pH Orion triode electrode with an Ag/AgCl internal reference.

XRD. Powder X-ray diffraction patterns were collected on a Siemens D5000 diffractometer. The instrument was equipped with a Ge fully focusing primary monochromator (Cu $K\alpha_1$ radiation, $\lambda = 1.540560$ Å) and a Brown 16° position sensitive flat PSD detector. The step size used was 0.0160° (step time 1.0 s) and the scan range was 3−40° (2θ).

Results

Previous results from in situ XRD and in situ ^{13}C NMR pH measurements were reported in two recent parent papers.[44,47] The strategy used to unravel the different chemical steps of SAPO-34 formation has been split into four different routes: synthesis of (a) triclinic SAPO-34 from a gel in the presence of HF and (b) trigonal SAPO-34 from a gel in the absence of HF. In (c), the synthesis was carried out as in route (a) but without silicon to investigate its possible role (producing triclinic $AlPO_4$-34), and at last, (d) synthesis of triclinic $AlPO_4$-34 from a slurry containing the prephase and water. These four different strategies bring complementary information on the synthesis processes.

NMR synthesis parameters are summarized in Table 1. It should be noted that the spectra from each nucleus were recorded from separate experiments, except in the synthesis of triclinic $AlPO_4$-34 from gel route (c). In all experiments, the maximum synthesis temperature was 170 °C and the syntheses were terminated after 4−5 h. An overview of the NMR spectra recorded from the different systems and nuclei is provided in Figure 2. The degree of crystallization for each sample was determined by comparison of ex situ X-ray diffraction patterns of the final products and the crystallization curves obtained in the in situ X-ray study.[44] In this study, focus was devoted to syntheses in the presence of HF. Results recorded in the absence of HF—route (b)—are included in Figure 2; however, more detailed spectra are provided as Supporting Information (see Figures 1S and 2S in the Supporting Information). They confirm the main kinetic regime of the intermediate prephase formation.

(45) Gerardin, C.; In, M.; Taulelle, F. *J. Chim. Phys. Phys.-Chim. Biol.* **1995**, *92*, 1877.
(46) Van Geet, A. L. *Anal. Chem.* **1968**, *40*, 2227.
(47) Vistad, Ø. B.; Akporiaye, D. E.; Taulelle, F.; Lillerud, K. P. *Chem. Mater.* **2003**, *15*, 1650−1654.

Table 1. Summary of the in Situ NMR Syntheses Parameters and the Products Formed[a]

nuclei	synthesis route	synthesis time (min)	product[b]	crystallization % CHA-type
^{19}F	(a)	245	SAPO-34 + prephase	∼55
^{27}Al	(a)	240	SAPO-34 + prephase	∼50
^{31}P	(a)	300	SAPO-34 + prephase	∼60
^{27}Al and ^{31}P	(b)	720	SAPO-34 + amorphous	NA
^{19}F, ^{27}Al, and ^{31}P	(c)	240	$AlPO_4$-34 + prephase	∼50
^{27}Al	(d)	175	$AlPO_4$-34 + prephase	90
^{31}P	(d)	205	$AlPO_4$-34 + prephase	>∼98

[a] All experiments were carried out with a maximum temperature of 170 °C. [b] The products contain some prephase because the syntheses were terminated before completion.

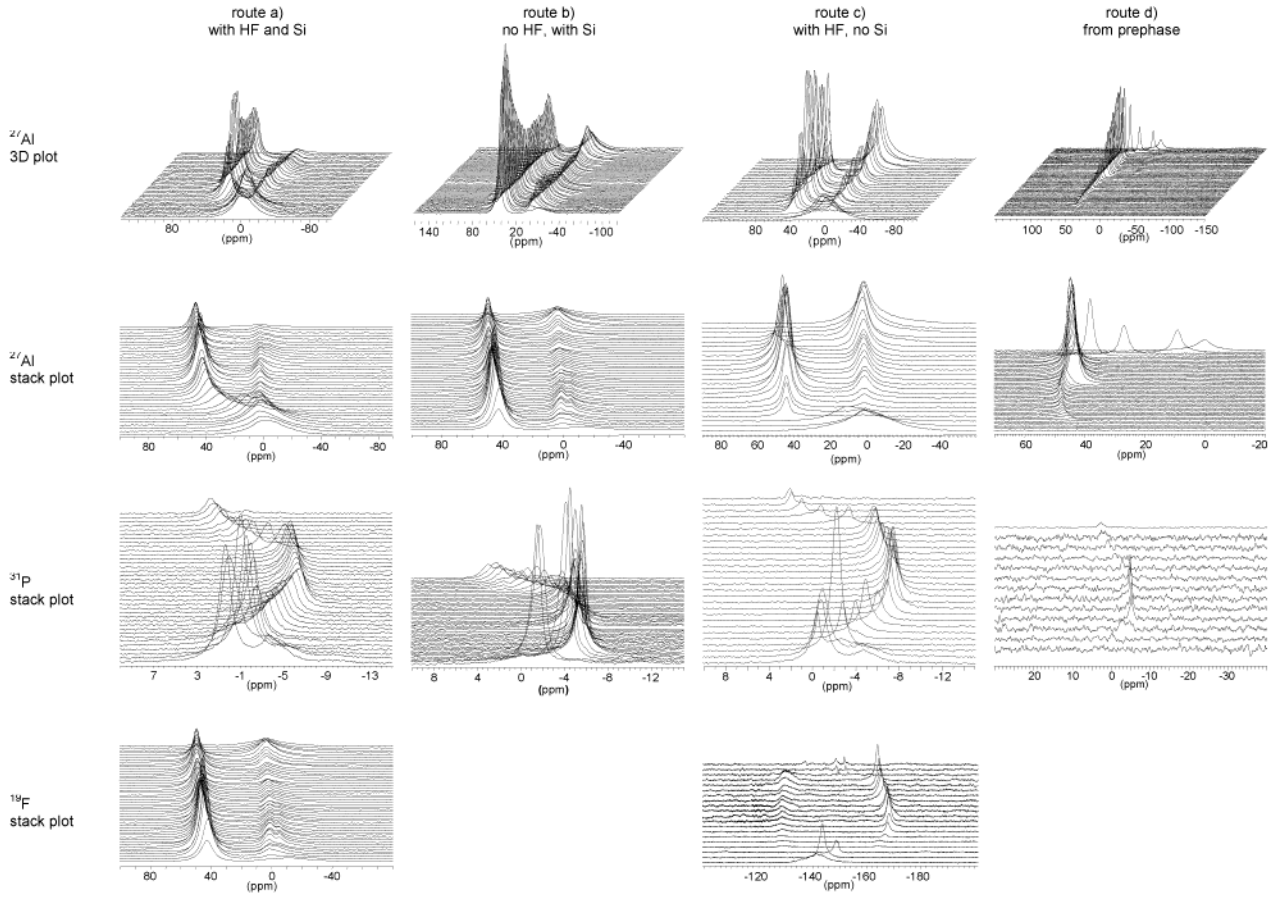

Figure 2. An overview of the NMR spectra recorded from the four synthesis routes investigated. The ^{27}Al spectra are displayed as both 3D and stack plots, the former demonstrating the intensity evolution, whereas the latter illustrates the chemical shift variations.

Ex situ pH measurements of the synthesis gel after mixing and after the hydrothermal treatment at 180 °C in a 50-mL Teflon-lined steel autoclave displayed an overall pH increase from ∼5.5 to ∼8.6 in the course of the synthesis. In situ ^{13}C NMR has been used in a parallel study to measure the pH throughout the synthesis,[47] uncovering a two-step pH profile. The first increase, from 5.5 to 7.3, took place during the formation of the prephase (95−120 °C). A minimum temperature of ∼160−165 °C was required to "initiate" the second pH increase from 7.3 to ∼8.6. This temperature corresponds to the minimum synthesis temperature needed to form the triclinic SAPO-34 phase in conventional 50-mL steel autoclaves (within reasonable time).[44] The pH remained essentially constant during the crystallization and the cooling stages, at about 8.6.

SAPO-34: In Situ NMR of the Synthesis from a Gel−Routes (a) and (b). *In Situ ^{27}Al NMR.* The in situ ^{27}Al NMR signal as a function of synthesis time is displayed in Figure 3. Only a broad signal in the region of hexacoordinated Al is observed at room temperature, in both situations, before and after the hydrothermal treatment. Prior to heating, the hexacoordinated signal exhibits a weak splitting that can be decomposed as the sum of two overlapping peaks at $\delta = 2$ and -10 ppm. To assign the chemical shifts to known coordination spheres, NMR spectra of model solutions composed of all the possible combinations (32 combinatorial different solutions) were prepared and examined at room temperature.[26] From these results, the peaks can be assigned to hexacoordinated fluoroaluminophosphate complexes. The exact composition of the coordination sphere cannot yet be fully elucidated from such a strategy, even if the type of ligand in the coordination sphere is predicted to be limited to fluoride, phosphate, hydroxide, and water.

The signal intensity increases during the first stage of the heating ramp are ascribed to solubilization of the

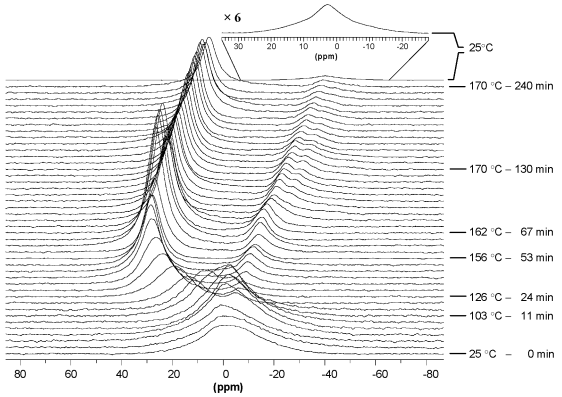

Figure 3. In situ ^{27}Al NMR spectra recorded during synthesis of triclinic SAPO-34 (*x*-scale increase between each scan = 1 ppm).

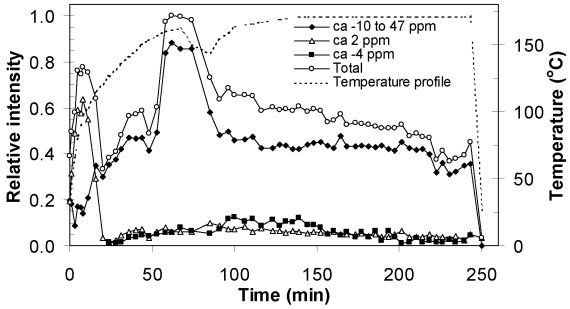

Figure 4. ^{27}Al NMR intensity as a function of temperature and time during synthesis of triclinic SAPO-34.

$Al(OH,F,H_xPO_4)_3$ gel (Figure 4). At intermediate temperatures (100−120 °C), a sharp drop in the intensity of the hexacoordinated Al occurred, whereas a peak in the region of 40−50 ppm appears. The region around 50 ppm is an ambiguous region for assignment to a five- or four-coordination state of aluminum. It has been shown that, for a mixed fluorophosphate species, at pH close to neutrality, the most likely assignment is pentacoordination.[10,11] Compared to the kinetics of formation obtained from in situ XRD capillary synthesis,[44] this coordination change takes place at the same temperature as the formation of the prephase.

After about an hour of heating, the temperature approached 165 °C. An increase in concentration of Al in the liquid phase is observed, followed by a noticeable decrease, with a gradual peak shift from 0 to 45.5 ppm (Figure 3). As nucleation needs a higher degree of supersaturation, this increase in concentration followed by a decrease may be ascribed to nucleation induction associated to a buildup of supersaturation. The crystal growth process takes over after this ∼30-min period of high supersaturation.

The amount of pentacoordinated Al remains almost constant during the crystal growth period, whereas some decrease of the small hexacoordinated aluminum site is detected. A small linear downfield shift (∼0.9 ppm/h) is monitored during the crystallization period, which may be an effect of the reduced concentration of hexacoordinated aluminum and rapid chemical exchange between the Al species in the solution. The main peak shifts with temperature during the cooling stage from ∼50 to 0 ppm. This is due to the reversible coordination change with temperature. No sign of pentacoordinated aluminum is detected at room temperature.

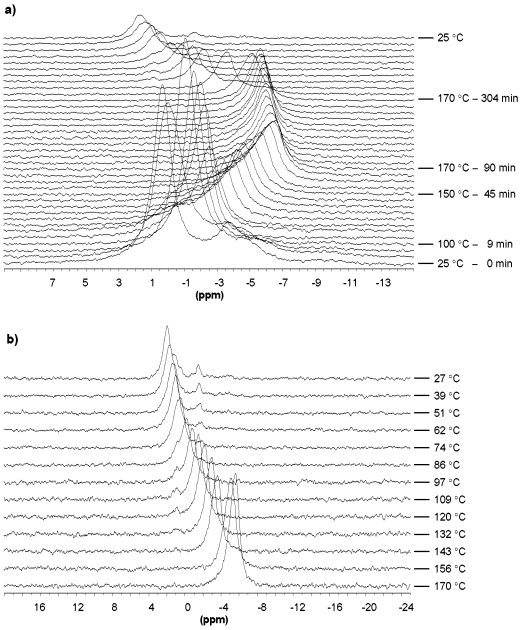

Figure 5. In situ ^{31}P NMR spectra (a) recorded throughout the synthesis of triclinic SAPO-34 and (b) selected spectra recorded during the cooling period (*x*-scale increase between each scan = 0 ppm).

In Situ ^{31}P NMR. The in situ ^{31}P NMR signal as a function of synthesis temperature and time is displayed in Figure 5. Prior to heating, three peaks are observed, the most intense peak ($\delta \sim 0.3$ ppm) being assigned to free phosphates undergoing chemical exchange with fluoroaluminophosphate species. The exchange is confirmed by the broadening of the signal and the high-field shift compared to those of a pure phosphate solution. The two other peaks, of medium and weak intensities at respectively −3.75 and −9.7 ppm, represent fluoroaluminophosphate and aluminophosphate complexes. At an initial pH ∼ 5.5, roughly all of the free phosphates (∼98%) are calculated to be in the diprotonated state $H_2PO_4^-$.

During the first stage of the heating, the main peak at 0.3 ppm shifts upfield, whereas the two peaks at −3.75 and −9.7 ppm disappear completely between 80 and 100 °C due to an increased rate of chemical exchange at higher temperatures. Thus, the main peak represents the weighted average of all the phosphate species present in the solution. The chemical shift variation of the main peak is plotted as a function of temperature and time in Figure 6, whereas the evolution of the intensity is displayed in Figure 7. The chemical shift exhibits a strong dependency on temperature and concentration. During the heating (at ∼100 °C), a smaller peak appears in the spectrum at about 0 ppm, corresponding to the intersection between the slopes in Figure 6, and may be related to the formation of the prephase. As the temperature approaches 170 °C, a minimum in the ^{31}P NMR chemical shift is observed, the overshoot beyond the stationary chemical shift during crystallization, being characteristic of supersaturation. Throughout the crystallization period, a continuous downfield shift is monitored. A linear correlation between the total ^{31}P intensity and the chemical shift variation is identified, indicating an increased proportion of free phosphate in the liquid phase.

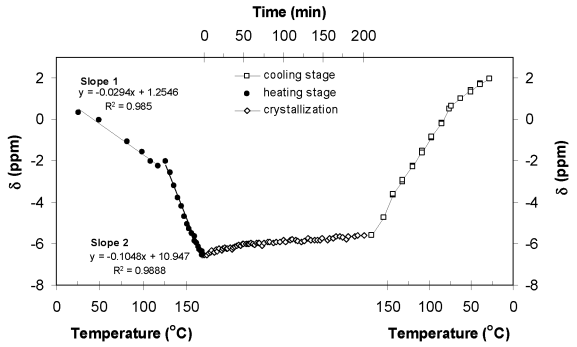

Figure 6. In situ ^{31}P NMR chemical shift of the main peak recorded during the heating and cooling stage as a function of temperature and the crystallization period as a function of time.

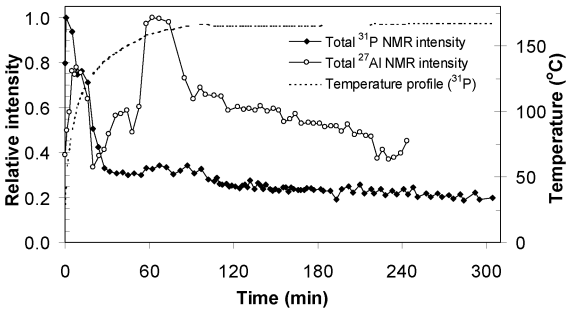

Figure 7. ^{31}P NMR intensity as a function of temperature and time during synthesis of triclinic SAPO-34. The heating profile and the total ^{27}Al NMR intensity are included as well.

For a better overview, the spectra recorded during the stepwise cooling period are also presented separately in Figure 5b. The downfield chemical shift of the main peak is a direct consequence of the temperature variation. The resolution increases drastically when the temperature is reduced and fast chemical exchange precludes the direct observation of the diversity of species at higher temperatures. When the number of scans is increased, at least 10 peaks can be observed after the solution is cooled to room temperature or in the mother liquid after synthesis is performed in conventional autoclaves (see Figure 3S in the Supporting Information). The fast exchange between many species is therefore confirmed at synthesis temperature. These peaks are most evident in aluminophosphate solutions at room temperature, appearing upfield of the free phosphate as in Figure 4b at 27 °C. They were observed as sharp peaks by Mortlock et al. only in the neutral region.[36,37] An extensive study would involve a systematic change of concentrations, temperature, pH, and Al/P ratio to assign all these peaks.

In Situ ^{19}F NMR. The in situ ^{19}F NMR spectra are displayed in Figure 8. Identical chemical shift behavior is observed in the absence of silicon in the gel (see Figure 4S in the Supporting Information). The broad peak observed prior to heating is assigned to the fluoroaluminophosphate complexes according to the results obtained from the model solutions.[26] The observed chemical shift of the main peak as a function of temperature throughout the heating and the cooling stages is displayed in Figure 9.

When the temperature is increased, the amount of observable fluorine first increases (Figure 10), indicating solubilization of fluorides from the gel. The chemical

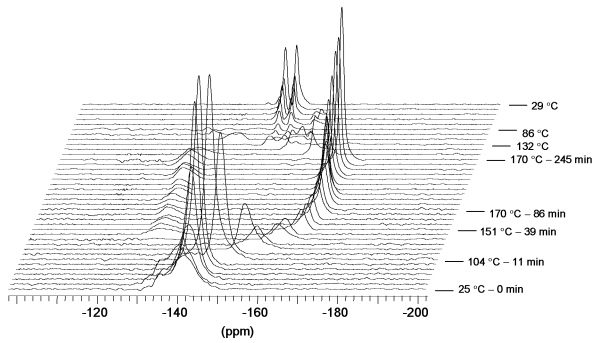

Figure 8. In situ ^{19}F NMR spectra recorded during synthesis of triclinic SAPO-34 (*x*-scale increase between each scan = 0.5 ppm).

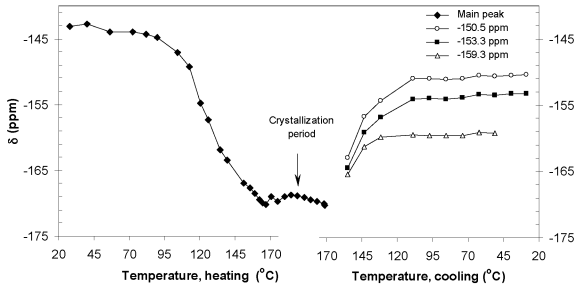

Figure 9. In situ ^{19}F NMR chemical shifts as a function of temperature during formation of triclinic SAPO-34. The left- and right-hand sides represent the heating and cooling stages, respectively. Only the main peak and the subsequent splitting during the cooling stage are included.

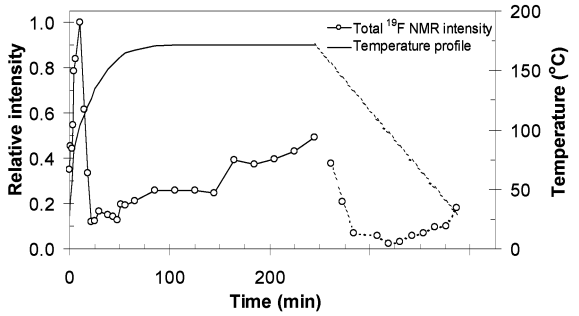

Figure 10. Total ^{19}F NMR signal intensity as a function of temperature and time during in situ synthesis of triclinic SAPO-34 (the time scale during the cooling stage is adjusted to give a linear correlation with the temperature—dotted lines).

shift profile, the intensity evolution of the main fluorine peak, and the trace of a small invariant signal at about −130 ppm are almost mirror images of the ^{27}Al spectra evolution, and are due to the coordination change of aluminum. The intensity decrease when the temperature approaches 100 °C is due to the formation of the prephase. The almost invariance in position and slight intensity change of the fluorine signal at −130 ppm allow assignment of this signal to the hexacoordinated aluminum species resonating around 0 ppm in ^{27}Al. This minor peak was also observed in the absence of silicon in the gel, implying that it does not originate from a silicofluoride.

Throughout the crystallization period, the intensity of the ^{19}F peak increases as a function of time since fluoride is released when the "fluoride-rich" prephase (F/[Al + P + F] ratio = 1/3) dissolves and the "fluoride-poor" triclinic SAPO-34 (F/[Al + P + Si + F] ratio =

1/7) forms. No significant shift in the peak position is detected during this period and the main peak stabilizes around −169 ppm.

During the cooling stage, a splitting of the main peak occurs (T < 155 °C), giving three separate peaks (δ = −151.1, −154.0, and −159.5 ppm at 97 °C). With cooling to room temperature, the two former peaks shift downfield to −150.4 and −153.3 ppm, whereas the latter disappears. These peaks, a few ppm downfield compared with those of the AlF_x^{+3-x} species,[26] are due to the AlF_xP_y coordination sphere. A sharp intensity decrease occurs between 170 and 132 °C, followed by a subsequent slow increase of the intensity for temperatures lower than 132 °C. The intensity loss is a reverse effect of the intensity increase observed during the heating stage and is due to precipitation of aluminum- or aluminophosphate-containing fluorides. A similar intensity loss is observed by in situ ^{19}F NMR during the formation of $AlPO_4$-34 from silicon-free gel (see Figure 4S in the Supporting Information).

$AlPO_4$-34: In Situ NMR Synthesis from Gel, in the Absence of Silicon—Route (c). Due to the short synthesis time and the low sensitivity combined with long acquisition time, it was not possible to record ^{29}Si NMR spectra within a suitable time frame. Therefore, to investigate the effect of silicon in the syntheses from gels, an in situ NMR synthesis in the absence of silicon was performed (Figure 2 or see more details in Figures 4S−6S in the Supporting Information). The resulting spectra were compared with those recorded in the presence of silicon. Ex situ powder X-ray diffraction of the final product confirmed formation of the prephase and approximately 50% transformation to $AlPO_4$-34 (Table 1).

Compared to the silicon-containing syntheses, two main differences are observed in the ^{27}Al spectra (see Figure 5S in the Supporting Information). First, the high degree of supersaturation observed in the presence of silicon when the final temperature is approached, is absent. Second, in the presence of silicon, a weak splitting of the hexacoordinated Al signal is observed at high temperature, which is not the case without silicon. The first observation may be due to the lower activation energy generally noticed for the formation of $AlPO_4$s compared with that for SAPOs.[44] Similar concentration profiles have been reported for the formation of the silicon-free ULM-3, ULM-4, and $AlPO_4$−CJ2 phases investigated by in situ ^{27}Al NMR.[11] The second observation should be related to differences in species, involving silicon in the second sphere of coordination of the hexacoordinated aluminum. The ^{31}P NMR spectra are similar to those recorded from the SAPO gels, except for a steeper downfield chemical shift as a function of time at high temperature and a faster intensity decrease, also at high temperature. Both these effects may be correlated to a reduced activation energy of $AlPO_4$-34 formation, compared to SAPO-34, and therefore a faster crystal growth. Only a minor difference is detected in the ^{19}F NMR spectra when the spectra recorded in the absence and the presence of silicon are compared. In the absence of silicon, a small continuous linear downfield shift of the main peak is observed during the crystallization period, whereas no such variation occurs when silicon is present.

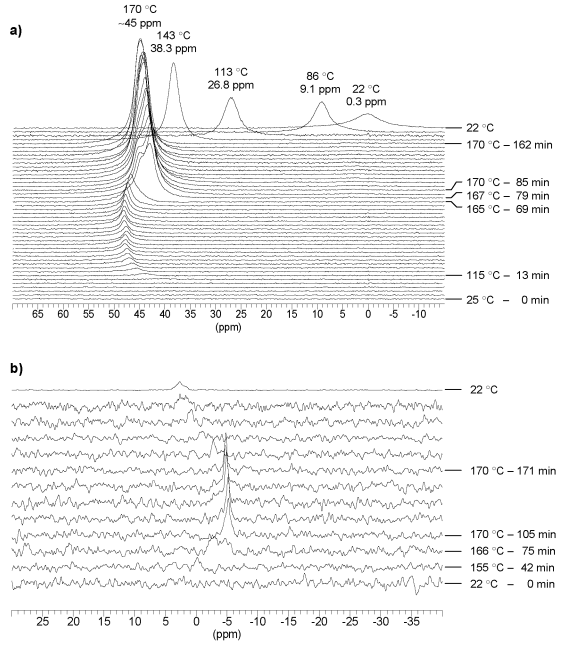

Figure 11. In situ NMR spectra recorded during formation of $AlPO_4$-34 from a prephase−water slurry: (a) ^{27}Al and (b) ^{31}P NMR (x-scale increase between each scan = 0 ppm).

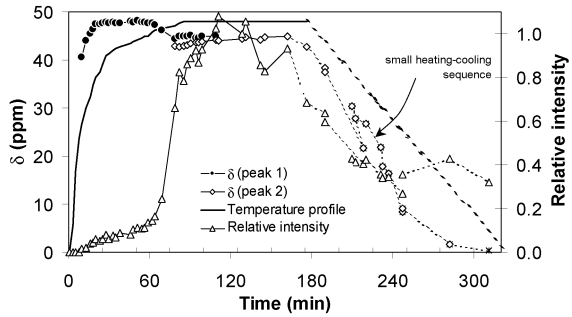

Figure 12. ^{27}Al NMR chemical shift and intensity extracted from the spectra recorded during formation of $AlPO_4$-34 from a prephase−water suspension (the time scale during the cooling stage is adjusted to give a linear correlation with the temperature—dotted lines).

AlPO-34: In Situ NMR Synthesis from the Prephase−Water Slurry—Route (d). We have shown in a previous contribution[44] that a slurry of the prephase and water can be used to prepare triclinic $AlPO_4$-34 by hydrothermal treatment. Compared to the original gel, the complexity of the solution is significantly reduced. Both prior to and after the hydrothermal treatment, a pH of ∼7.5 ± 0.25 is measured ex situ with a pH meter. The results were confirmed by in situ ^{13}C NMR recordings at high temperature.[47] No significant variations of the ^{13}C chemical shifts were detected.

In situ ^{27}Al and ^{31}P NMR spectra recorded during the two separate syntheses are displayed in parts a and b, respectively, of Figure 11. The ^{27}Al NMR chemical shifts and intensities throughout the synthesis are summarized in Figure 12. The prephase is insoluble at room temperature, and no signals are detected for any of the nuclei before heating. During the heating stage, a weak ^{27}Al signal appears around 40 ppm when the temperature reaches 95−105 °C. With further temperature increase, the Al signal shifts downfield and its intensity increases as the prephase dissolves. When the temper-

ature approaches 170 °C, (a) a splitting of the peak, (b) a sharp increase of the intensity, and (c) an upfield chemical shift are observed. The slurry contains all the species necessary for the formation of triclinic $AlPO_4$-34. The ^{27}Al upfield shift from ∼45 to 0 ppm during the cooling stage is ascribed to the coordination change of aluminum, from 5 to 6, induced by temperature.

Correspondingly, a noisy ^{31}P NMR signal appeared when the temperature reached ∼115 °C. The signal followed roughly the same course as that observed from the gel system; however, the spectra are noisy due to the low concentration of phosphorus.

Discussion

The discussion of this in situ NMR study is strongly related to the in situ X-ray powder diffraction study[44] and to the in situ ^{13}C NMR pH measurement of the identical system.[47] Since the major objective behind the XRD study was to examine the kinetics of formation, the initial temperature ramping was performed as rapidly as possible. However, with rapid heating, a two-stage heating profile (Figure 1) was needed to obtain the pure CHA-like phase within the 0.5-mm quartz capillaries. An identical heating profile could not be strictly reproduced within the larger hydrothermal NMR tube. Nevertheless, when the evolving species is related to the applied heating profile, the trends obtained from XRD and NMR can be compared as displayed in Figure 13. The upper left-hand side represents the heating stage as a function of temperature, whereas the upper right-hand side displays the observations as a function of time under synthesis conditions.

Prior to heating, the system contains some hexacoordinated fluoroaluminophosphate and aluminophosphate complexes in solution, the amorphous $Al(OH,F,H_xPO_4)_3$ gel, some silicon-containing compounds, and morpholine. Some unreacted Al source may also be present. The pH is 5.5, and as expected from the equilibrium constants,[48] the amount of observable aluminum in solution is low.

During the first stage of the heating (T < ∼95 °C), the amounts of observable aluminum and fluorine increases as a function of temperature, indicating progressive solubilization of the amorphous phase. ^{19}F NMR parallels ^{27}Al in terms of intensity, supporting the assumption that the species formed during the gel dissolution contains Al−F bonds. Simultaneously, the ^{31}P intensity in solution is essentially unchanged, indicating an increase of the P/Al ratio in the remaining amorphous phase (the total intensity variations of the various nuclei are displayed in Figure 13).

The pH increases in two steps.[47] The first increase from 5.5 to 7.3 takes place during the formation of the prephase. Simultaneously, a large reduction of aluminum, phosphorus, and fluorine concentrations is monitored by NMR. A second pH increase up to 8.6 occurs when the synthesis temperature (160−165 °C) is approached.

When the temperature increases, aluminum changes its coordination from hexacoordinated at room temperature to pentacoordinated at temperatures higher than 150 °C, as monitored by its downfield chemical shift (Figure 3). The pH variations[47] may allow the coordination change. Hexacoordinated aluminum, in an acidic medium, gives rise to signals in the −20 to 20 ppm range, whereas tetracoordinated aluminum, in basic solutions, produces signals in the 40−80 ppm range depending on the ligands. A "neutral pH" (±1.5 around the $pK_w/2$) allows coexistence of coordination states in the presence of fluoride as a ligand. In the absence of fluoride, aluminum would be hexacoordinated or tetracoordinated at room temperature. In the presence of fluoride, aluminum in 5-fold coordination would be stable in water over a range of about 3 units of pH, around neutral.[10,11] Therefore, the coordination change observed for aluminum can be attributed to either the pH increase alone or the temperature variations during the synthesis. Actually, the pH increases from about 5.5 to 8.6 during the synthesis—route (a)—and only hexacoordinated aluminum is observed at pH = 8.6 after cooling to room temperature. For that reason, the pH is probably not the origin of the coordination change. The most likely explanation is that, in full analogy with previous work of Taulelle et al.,[10] the temperature induces a loss of water in the coordination sphere. At neutral pH, and close to it, the five-coordination range of stability opens, between about 5.5 and 8.5, and coexistence of the five-coordination may occur with six- or four-coordination. Such arguments and observations were previously presented by Haouas.[11]

An electrostatic energy calculation study based on a "partial charge" approach[49] has been carried out by Taulelle et al.[10,11] A case study has been examined, the formation of microporous $AlPO_4$−CJ2 in a fluoride medium at neutral pH by in situ multinuclear NMR. Calculations support the assumption that the coordination change is due to a loss of a water molecule between the six- and five-coordinated Al species. A good candidate for the pentacoordinated Al first coordination sphere is $[Al(OPO_3H_2)F_x(OH)_{3-x}(H_2O)]^-$.

The formation of the layered $AlPO_4F$ phase takes place between 95 and 125 °C, as indicated in Figure 13b and by in situ XRD. This observation is correlated to (a) the reduction of the ^{27}Al, ^{31}P, and ^{19}F NMR intensities, (b) the fast exchange of NMR peaks for ^{31}P nuclei, and (c) the change in the displacement rate of the ^{27}Al, ^{31}P, and ^{19}F chemical shifts as a function of temperature, induced by the coordination change of aluminum.

The high degree of supersaturation of aluminum occurs simultaneously as the pH increases to 8.6. It is reasonable to assume that nucleation of SAPO-34 is activated by this supersaturation and that the supersaturation is a result of the second pH increase.

^{27}Al coordination and speciation are the most critical steps of the spectral assignment. First, at room temperature, the coordination of aluminum in solution is six. Thus, aluminum contains fluoride and phosphate in its coordination sphere in addition to water and hydroxide. These species would not be expected to be monomeric; particularly, the NMR peak widths would be narrower. Since they are issued from a gel containing condensed species, dimers or trimers are expected. The fluorophosphate species in solution are not more con-

(48) Hansen, E. W.; Vistad, Ø. B.; Akporiaye, D. E.; Lillerud, K. P.; Wendelbo, R. *J. Phys. Chem. A* **1999**, *103*, 2532.

(49) Henry, M.; Merceron, T. *Radiochim. Acta* **1994**, *66/67*, 57.

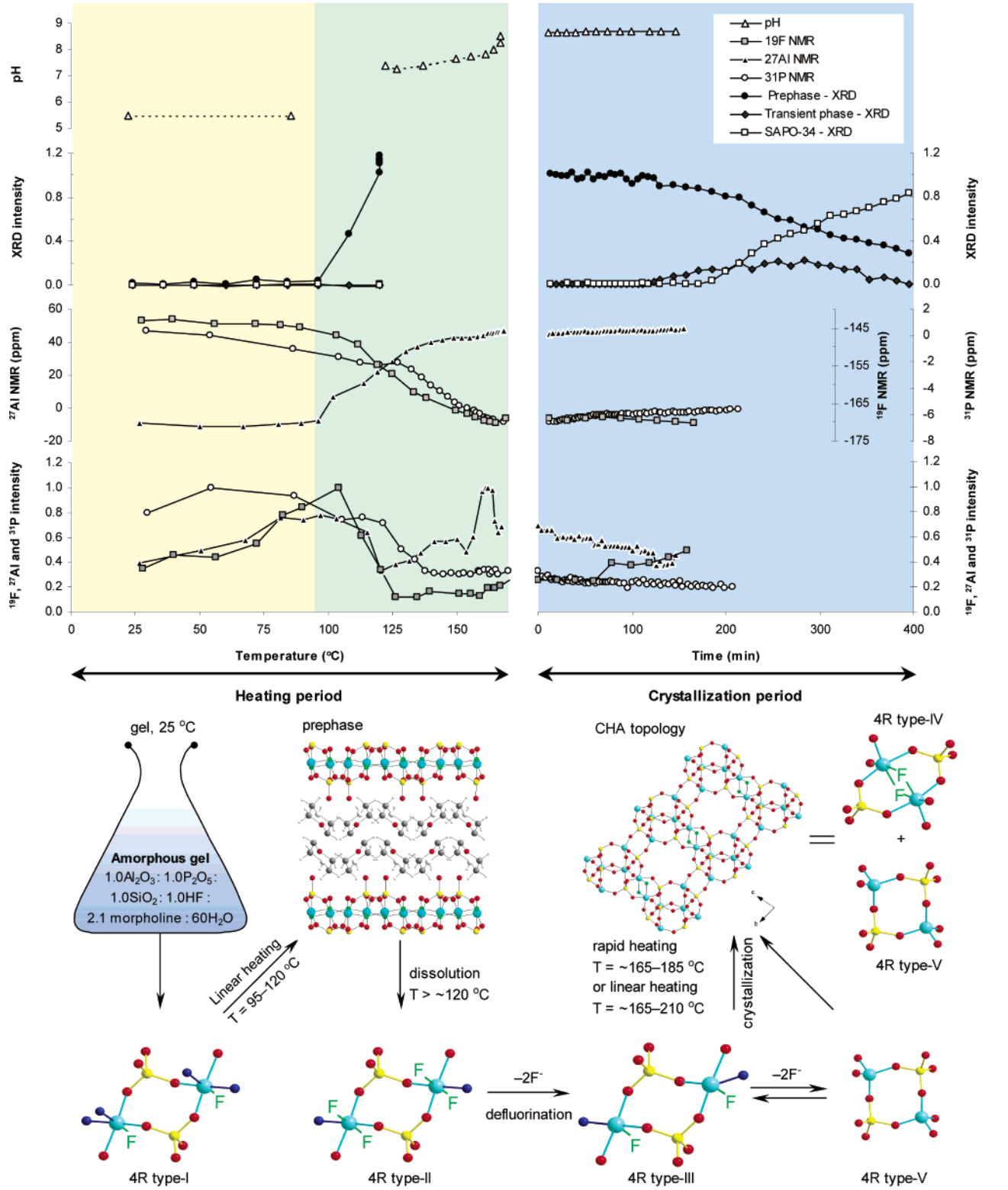

Figure 13. Information obtained from in situ NMR and in situ XRD analysis of the hydrothermal formation of SAPO-34. The two upper left-hand columns represent the heating period, whereas the upper right-hand column displays observations made under synthesis conditions. Time-zero corresponds to the moment when the final synthesis temperature (170 °C) was achieved. No X-ray observations are displayed between 120 and 170 °C due to the heating profile applied (no. IV with maximum temperature = 169 °C).[44] In the lower part, a schematic overview of the proposed synthesis mechanism is presented, including the most important equilibriums and synthesis parameters.

densed than 4R units. More condensed species, double 4-rings (D4R) or double 6-rings (D6R) are considered unlikely with morpholinium cation. Its rather high charge density precludes very large counteranions. Actually, morpholine with a pK_a of 8.78 has a charge density quite comparable to NH_4^+ ($pK_a = 9.25$ but with a smaller size than morpholine). The relation between charge density derived from Ferey's work[50] allows us

(50) Ferey, G. *J. Fluorine Chem.* **1995**, *72*, 187.

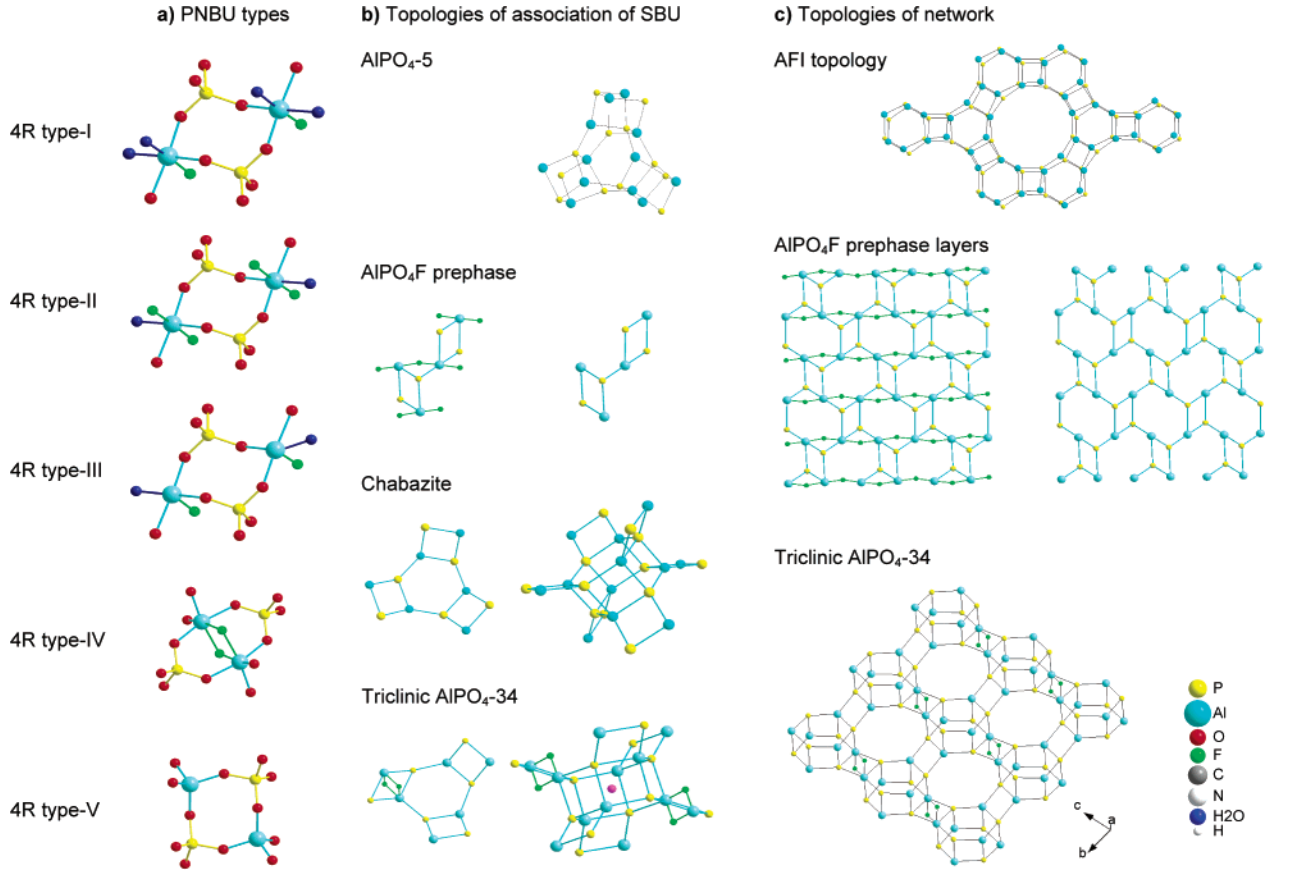

Figure 14. (a) 4R types involved in the syntheses, (b) topologies of 4R assembling in crystals, and (c) crystalline framework topologies of the crystals considered in this work.

to deduce that the size of the condensed species for the protonated morpholine with a pK_a of 8.78 cannot be greater than 4R. 6R, D4R, or D6R would require pK_a on the order of 10−12 for having a charge density sufficiently low to match the low charge density of the larger units. As all structures characterized by XRD in the preceding study contain four rings (4R) only, we do not consider six rings (6R) as being of large importance in these solutions, even if a stacking of double 6-rings is the normal method for illustrating the CHA topology. Therefore, we can assume 4R species of types I or II depending on the amount of fluoride per aluminum (see Figure 14).

A critical observation can be made of synthesis (d) carried out from the prephase. No signal appears before the onset of prephase dissolution, at about 120 °C. After this temperature, one ^{27}Al NMR signal appears, with a characteristic evolution that is the same as the signal observed in synthesis (a) after the redissolution of the prephase. This signal may represent a prenucleation building unit (PNBU) in the sense of Taulelle.[51,52] The sharp intensity increase provides the necessary supersaturation for nucleation of the triclinic $AlPO_4$-34. Considering the structure of the prephase as sketched in Figure 14c, a candidate for the PNBU that can easily be extracted from the prephase is a 4R unit of type II. However, as it contains one fluorine per aluminum, and its coordination changes from six to five as monitored by its chemical shift, one can assume an extraction of a 4R type II that will expel two fluoride anions to eliminate the charge excess and leave aluminum at five-coordination (4R type III) due to the temperature that favors this environment.

A fast dynamic exchange process takes place at all temperatures, from 20 to 150 °C, in syntheses (a), (c), and (d). The observed ^{27}Al peak position represents the averaged chemical shift of the five and six-coordinated Al species and the equilibrium between these two compounds is reversibly linked to the temperature. However, surprisingly, this exchange does not involve all aluminum species. Two hexacoordinated aluminum species are present without exchange in syntheses (a) and (b) and one such signal in synthesis (c). As no such signal appears in synthesis from the prephase (d), these hexacoordinated species are formed initially and do not rapidly interconvert to 4R units of type III.

The concentration of aluminum in solution parallels the pH evolution when the temperature approaches 170 °C. It is reasonable to propose that the increase of aluminum concentration caused by the second pH increase produces a supersaturation of 4R units of type III that rearrange in types IV or V, inducing nucleation of the SAPO-34 phase. The prephase continuously dissolves as the SAPO-34 phase is formed. This transformation mechanism is confirmed in the in situ X-ray study by the partial dissolution of the prephase as a function of temperature when the temperature was increased directly from 120 °C to the synthesis temperature.[44] Thus, the crystal growth proceeds by a liquid−solid mechanism.

(51) Taulelle, F. *Curr. Opin. Solid State Mater. Sci.* **2001**, *5*, 397.
(52) Taulelle, F. *Solid State Sci.* **2001**, *3*, 795.

Without first the formation of the crucial prephase, only the formation of SAPO-5 (AFI topology) was observed by in situ XRD.[44] Because of the low activation energy of $AlPO_4$-5 formation,[53] a competition takes place between formation of SAPO-34 and the AFI topology when the gel is heated quickly from room temperature to the desired synthesis temperature (within 2 min). The activation energy of $AlPO_4$-5 formation is expected to be comparable to that of the prephase due to the symmetry of the network that can be built up by simple stacking of the nonfluorinated 4R type-I units (Figure 14). These units allow for easy loss of water and coordination lowering to four. Thus, the key role of the prephase might be as a continuous source of fluoride containing PNBU units during the crystallization period as the prephase dissolves.

The SAPO gels contain a large amount of silicon. However, it was not possible to record in situ ^{29}Si NMR spectra within a reasonable time frame. From synthesis (c) in the absence of silicon, most of the NMR spectral features are analogous to synthesis (a) except that, in the hexacoordinated region at high temperature, two lines are observed for (a) and only one for (c). Thus, the incorporation of silicon may proceed through the formation of a 4R type I where silicon has replaced one aluminum or phosphorus. Moreover, it seems feasible to predict for units without silicon a lower activation energy since $AlPO_4$-34 can be obtained without the high degree of Al supersaturation. This lower activation energy can be related to the coordination of aluminum that changes from six to five, allowing further condensation. When 4R units containing silicon in four-coordination and aluminum in six-coordination are stabilized, the condensation mechanism must undergo an elimination−addition mechanism on aluminum. For the case of lesser coordination, the elimination step has been already done; only the addition step is required and proceeds more easily.

In synthesis (b) without HF, the signal characteristic of formation of the $AlPO_4F$ prephase is absent, which is expected since there is no fluoride available to form the PNBU necessary to form the prephase.

At last in synthesis (d), only one peak appears at $\delta =$ 45 ppm in the ^{27}Al NMR spectra, representing 4R type-III units. The 4R type IV has no signature in the solution spectra. The bridging may happen at the nucleation and growth step as a clipping of the network into a crystal.[46]

Conclusion

In both the main cases examined (the use of an ordinary gel in the presence of HF and the prephase−water slurry), the triclinic form of SAPO/$AlPO_4$-34 is obtained as the final product. Identical trends are observed in the NMR spectra recorded from both systems, except during the initial heating stage at $T <$ 100 °C. From the achieved results, one can propose a mechanism of formation of the different phases, as sketched in the lower part of Figure 13.

The first step is dissolution of the gel, producing 4R type-I units. Increasing the temperature leads to the formation of the layered $AlPO_4F$ prephase out of these 4R type-I units by simple alternating stacking. This requires very low activation energy. The prephase redissolves at temperatures starting at 120 °C to give 4R type-II units. By defluorination, 4R type-III units are formed and the aluminum coordination changes from six to five. Maintaining the defluorinating process leads to equilibrium with 4R type-V units. Condensation of 4R types III and V leads to the triclinic CHA topology, with double fluorine bridging as the consequence of clipping the network into a crystal. A weak competition with another unknown transient phase involving the same units takes place but vanishes as chabazite takes over.

Finally, the incorporation of silicon may proceed by substitution of aluminum or phosphorus in the 4R type-I units. This leads to very high activation energy of integration of the 4R units because they need to eliminate and then add a connection, instead of adding only as in the case of silicon-free 4R type-I units. This mechanism can explain the gradual incorporation of silicon into the prephase as a function of synthesis time because the integration occurs through a constant redissolution−recrystallization process, involving 4R type-I units. Similarly, this mechanism explains the gradual incorporation of silicon into triclinic SAPO-34 that has been observed during the first 12 h of synthesis.[44]

Hydrothermal syntheses are difficult to analyze because of the extremely reactive and aggressive liquids involved. Additionally, the very heterogeneous nature of the mixtures containing gel, supersaturated solutions, and crystals makes the characterization of the syntheses almost an impossible task. However, a proper combination of in situ XRD and NMR puts the challenge in possible reach.

It has been shown in this contribution that the variety of phenomena involved in the synthesis of SAPO-34 can be described with a few species. The quite large variety of reactions involved are controlled mainly by the activation energy of the reactions, with the main controlling factors being pH, temperature, and the nature of the SDA, and among the aspects controlled by temperature, the coordination of aluminum is critical.

Compared to controlled organic synthesis, control of the activation energy is the leading parameter, and not the thermodynamics of bond formation, which provides very small differentiation.

Acknowledgment. The authors would like to acknowledge the financial assistance from the Research Council of Norway. Likewise, we would like to thank Chantal Lorentz for assistance with the in situ NMR sampling at “RMN et Chimie du Solide”, Université Louis Pasteur, Strasbourg, France.

Supporting Information Available: In situ NMR spectra recorded during (a) the synthesis of trigonal SAPO-34 (in the absence of HF) and (b) the synthesis of triclinic $AlPO_4$-34 (in the absence of silicon) are collected. Additionally, some in situ ^{31}P NMR spectra (with increased resolution) recorded during the cooling stage are provided (PDF). This material is available free of charge via the Internet at http://pubs.acs.org.

CM021317W

(53) Davies, A. T.; Sankar, G.; Catlow, R. A.; Clark, S. M. *J. Phys. Chem. B* **1997**, *101*, 10115.